JOURNAL OF MATERIALS SCIENCE 30 (1995) 1005–1008

Strengthening of silicon carbide by surface compressive layer

YOUNG-WOOK KIM, JUNE-GUNN LEE
Structural Ceramics Laboratory, Korea Institute of Science and Technology, P.O. Box 131 Cheongryang, Seoul, Korea

Silicon carbide ceramics containing 4.7 wt% WC and 0.3 wt% Co were fabricated by hot-pressing with various additives (B, AlN, and polycarbosilane). Addition of WC and Co liquid phase resulted in considerable increase in flexural strength up to 1085 MPa for the 1 wt% AlN, 0.5 wt% B, and 20 wt% polycarbosilane-added specimen. The improved flexural strength was a result of surface compressive layer. The surface compressive layer was introduced by the liquid flow phenomenon during hot pressing.

1. Introduction

Silicon carbide has been one of the most promising high-performance ceramics due to its excellent strength and oxidation resistance at elevated temperatures [1–3]. Several attempts to improve its strength and reliability have been reported, including grain boundary oxidation [4], the use of wet processing [5], the preparation of fine-grained materials from pyrolyzed polycarbosilane [6], and the use of transient liquids [7]. Another approach is to introduce surface compressive stresses that can contain strength-controlling surface flaws and can result in improvement of strength [8–10].

In this study, the establishment of a surface compressive layer was achieved using the liquid flow phenomenon in silicon carbide ceramics containing WC, Co, AlN, B and polycarbosilane.

The objectives of this paper are to report the occurrence of the liquid flow phenomenon in SiC–WC–Co–AlN–B–polycarbosilane composition and to fabricate high-strength silicon carbide with surface compressive layer using that phenomenon.

2. Experimental procedures

Solutions of polycarbosilane in hexane were prepared. Precalculated amounts of α-SiC powders were then impregnated with these solutions, dried, and pyrolyzed using a heating rate of 2 °C/min under argon with a 1 h hold at 1000 °C. The pyrolyzed powders were hydrofluoric-acid treated to remove SiO_2, which was present as an impurity of the α-SiC starting powder, and a pyrolysis residue of polycarbosilane. Co was added into the pyrolyzed and hydrofluoric-acid treated powders using a precalculated amount of reagent-grade $CoCl_2 \cdot 6H_2O$. The cobalt chloride was decomposed at 400 °C for 3 h in flowing hydrogen. The powder mixture of Co-doped SiC with various additives (AlN, B, WC) was milled in acetone with SiC grinding balls using a polyethylene bottle. The milled slurry was dried, sieved, and hot-pressed at 1950 °C for 30 min with 25 MPa applied pressure.

Densities were measured using the Archimedes principle. Flexural test samples were cut into 3 × 3 × 25 mm from hot-pressed disc samples, and their surfaces and edges polished with an 800-grit diamond wheel. Flexural strengths were measured at various temperatures by a four-point bending method. The flexural strength sample was investigated by scanning electron microscopy (SEM) and transmission electron microscopy (TEM). The thermal expansion coefficient and fracture toughness were measured for residual stress calculation. The fracture toughness was measured using a Vickers indenter with a load of 49 N.

3. Results and discussion

3.1. Liquid flow phenomenon

Earlier observations of liquid phase sintering of W–Ni compacts showed that liquid sometimes flowed into the specimen's interior, leaving a porous region near the surface [11]. This phenomenon has also been observed in W–Ni–Fe, Cu–Zn and Co–Cu powder compacts [12], and has been attributed to the reduction of the liquid-vapour interfacial area by forming a liquid agglomerate at the specimen centre [12].

Table I shows the occurrence of liquid flow in various specimens. The chemical composition of the pyrolysis residue of polycarbosilane was reported in previous work [13]. Only specimen PCS4 showed liquid flow into the interior, as shown in Fig. 1. The boundaries between inner and outer regions were seen clearly. The horizontal cross-section showed the same phenomenon. As shown in Fig. 2 at a higher magnification, the interior region had a lower porosity than the outer region adjacent to the specimen surface.

In the WC–Co phase diagram [14], the lowest melting point liquid appears at about 1280 °C. Hence, liquid formation during hot-pressing was obvious in the PCS4 specimen. For a more precise investigation of liquid formation during hot-pressing, the PCS4 specimen was investigated by TEM (Fig. 3). It shows the presence of a continuous grain boundary phase. For the liquid flow phenomenon to occur, the

0022–2461

TABLE I Occurrence of the liquid flow phenomenon in various specimens

Sample designation	Composition (wt %)	Density (g/cm^3)	Liquid flow
PCS0	α-SiC + 20polycarbosilane + 4.7WC + 0.3Co	2.99	No
PCS1	α-SiC + 20polycarbosilane + 4.7WC + 0.3Co + 1B	3.10	No
PCS2	α-SiC + 20polycarbosilane + 4.7WC + 0.3Co + 1Al	3.21	No
PCS3	α-SiC + 20polycarbosilane + 4.7WC + 0.3Co + 2AlN	3.21	No
PCS4	α-SiC + 20polycarbosilane + 4.7WC + 0.3Co + 1AlN + 0.5B	3.22	Yes

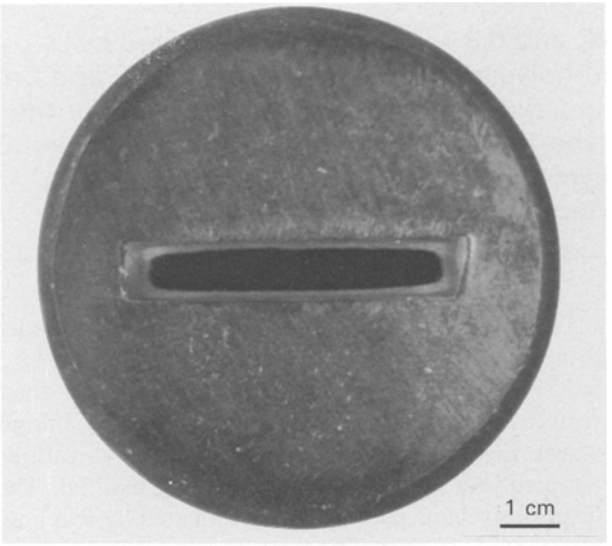

Figure 1 Vertical cross-section of PCS4 specimen.

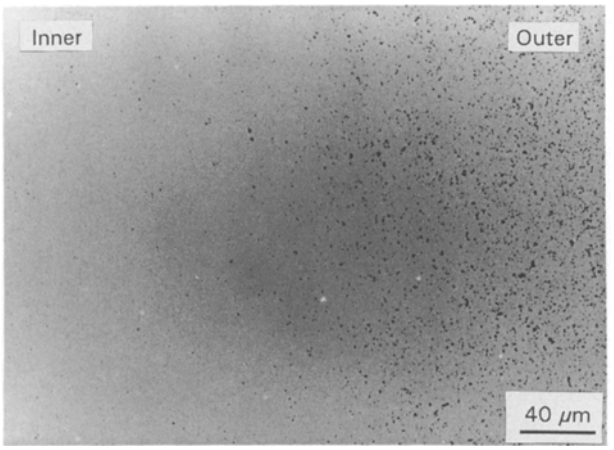

Figure 2 Microstructure of the same specimen as in Fig. 1 at a high magnification.

presence of a continuous liquid phase inside the specimen is a necessary condition [11]. Microanalysis using X-ray energy dispersive spectroscopy (EDS) on the outer and inner layers revealed 93.4 wt % Si, 5.3 wt % W, 0.5 wt % Co and 0.8 wt % Al for the inner layer and 95.5 wt % Si, 3.4 wt % W, 0.2 wt % Co and 0.9 wt % Al for the outer layer. B and C could not be analysed because of the limited sensitivity of the equipment. The above results show that the liquid phase was formed and flowed into the interior during hot-pressing, and may consist of Co and WC.

The effect of the addition of B and AlN on the liquid flow phenomenon is not clear but we can suggest the

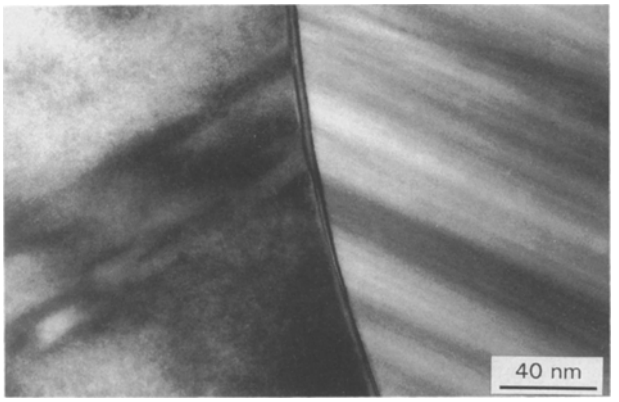

Figure 3 TEM micrograph showing continuous grain boundary phase.

following idea. Since B and AlN have solubilities in SiC [15, 16], the addition of B and AlN changes the surface energy of α-SiC which results in a change of the wetting angle of the liquid. The above discussion shows that some specific conditions must be satisfied for the liquid flow phenomenon to occur.

3.2. Mechanical properties

Three-layer bars with an outer layer thickness of 200–300 μm were prepared. To compare the room-temperature strength of each layer, the three-layer bars were cut into three bars and polished and chamfered with an 800-grit diamond wheel. The room-temperature strengths of each specimen are given in Table II, which shows that three-layer bars have a higher strength than one-layer bars. The five bars with an outer layer of 200–300 μm had a mean strength of 1085 MPa and a standard deviation of 129 MPa. One of the five bars failed because of chamfering while the other four bars failed because of internal flaws (large voids or large grain) near the interface between the inner and the outer layers (Fig. 4). However, two of the ten one-layer bars failed because of chamfering, one because of an internal flaw, and the other seven from the tensile surface. From the fracture surface observations, it is evident that surface flaws were responsible for the lower strength of the one-layer bars.

The fracture behaviour of the three-layer bars was quite different from that of the one-layer bars. Three-layer bars fractured into 5–12 pieces, while one-layer bars fractured into 2–3 pieces.

The fracture behaviour, strength, and fracture origin differential between one-layer bars and three-layer

TABLE II Comparison of room-temperature strength between one-layer SiC and three-layer SiC specimens

Specimen	Size (mm)	Flexural strength (MPa)
Outer layer	$3 \times 0.3 \times 25$	794 ± 120
Inner layer	$3 \times 2.5 \times 25$	951 ± 157
Three-layer[a]	$3 \times 3.5 \times 25$	1085 ± 129

[a] Three-layer bars with outer layers ~ 200–300 μm in thickness.

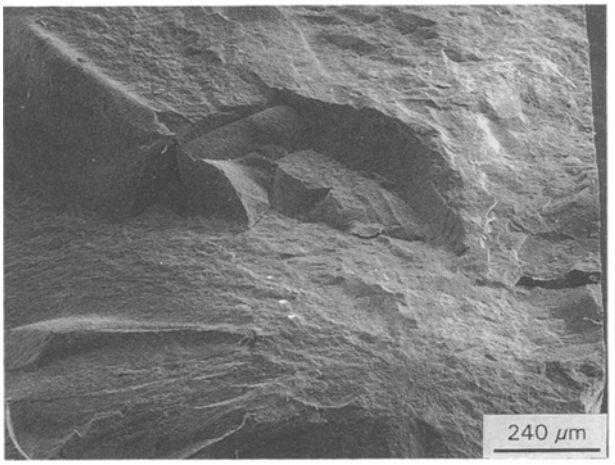

Figure 4 SEM fractography of three-layer SiC ceramics showing failure origin located at the compressive/tensile interface.

bars at room temperature gives an indication of the residual stress achieved, since failure generally occurred from the tensile surface in one-layer bars. The residual stress achieved is temperature-induced stress due to the thermal expansion coefficient differential between the outer and inner layers.

The expected compressive residual stress in the outer layer of the three-layer bars can be calculated from the following equation [17]:

$$\sigma = -[(E_1 E_2 d_2 \Delta T)(\alpha_2 - \alpha_1)]/[(1 - \nu)(E_1 d_1 + E_2 d_2)] \quad (1)$$

where E is Young's modulus, d is thickness, ΔT is the temperature difference over which stress exists, ν is Poisson's ratio, α is the coefficient of linear thermal expansion and the subscripts 1 and 2 refer to the outer and inner layers, respectively.

Taking E_1 as 425 GPa [18], E_2 as 460 GPa [18], d_1 as 250 μm, d_2 as 3000 μm, ΔT as 1300 °C, α_1 as 4.55×10^{-6}/°C, α_2 as 4.72×10^{-6}/°C and $\nu = 0.17$ [19], the expected compressive residual stress in the outer layer is 105 MPa.

The residual stress achieved in the three-layer bars could also be estimated using the expression derived by Marshall and Lawn [20]:

$$\sigma_r = [K_c/(\pi \Omega C_r)^{1/2}][1 - (C_0/C_r)^{3/2}] \quad (2)$$

where C_0 is the crack length in the unstressed material, C_r is the crack length in the stressed material either parallel or perpendicular to the interface, and Ω is the geometric constant ($\sim 4/\pi^2$).

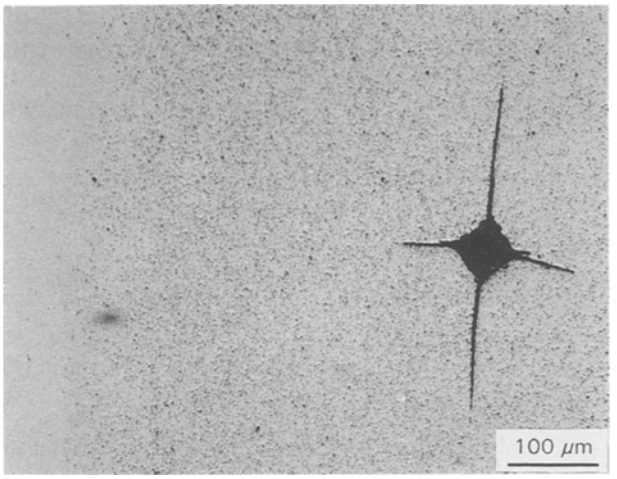

Figure 5 Optical micrograph of cross-section of three-layer SiC ceramics with indents oriented with cracks parallel and perpendicular to the interface/surface.

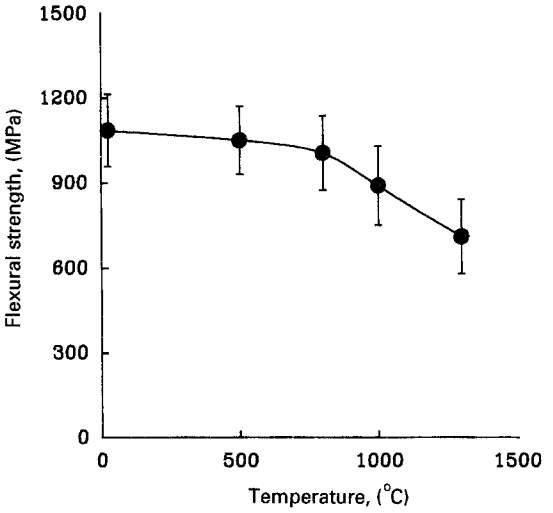

Figure 6 Dependence of strength on temperature for three-layer SiC ceramics.

By aligning cracks parallel and perpendicular to the surface and interface, it is possible to see longer cracks in the inner layer perpendicular to the interface and surface and shorter cracks parallel to the interface and surface (Fig. 5). Taking K_c as 3.0 MPa $m^{1/2}$, C_0 as 114 μm, C_r as 90 μm for the outer layer and 173 μm for the inner layer, the expected compressive residual stress in the outer layer is 118 MPa. This value is similar to the value calculated from Equation 1. The corresponding residual tensile stress in the inner layer is approximately 94 MPa. The above observations with indentation cracks and calculations explain why the strength of three-layer SiC ceramics is high.

The dependence of strength on the test temperature for three-layer bars is shown in Fig. 6. The three-layer bars show a rapid degradation in strength with temperature. The presence of liquid at high temperatures and the reduction of the thermal expansion coefficient difference between outer and inner layers with temperature could certainly be a possible reason for the degradation of strength with temperature.

4. Conclusions

1. The liquid flow phenomenon is observed in the α-SiC-20 wt %, polycarbosilane-4.7 wt %, WC–0.3 wt%, Co-1 wt %, AlN-0.5 wt %, B composition during hot-pressing.

2. Silicon carbide ceramics with surface compressive layer can be fabricated using the liquid flow phenomenon.

3. Typical flexural strengths of SiC ceramics with compressive surface layer at room temperature and 1300 °C are 1085 MPa and 710 MPa, respectively.

References

1. J. J. BURKE, A. E. GORUM and R. N. KATZ (eds), "Ceramics for High Performance Applications" (Brook Hill, Chestnut Hill, MA, 1974).
2. J. J. BURKE, E. N. LEONE and R. N. KATZ (eds), "Ceramics for High Performance Applications II" (Brook Hill, Chestnut Hill, MA 1977).
3. E. M. LEONE, R. N. KATZ and J. J. BURKE (eds), "Ceramics for High Performance Applications III" (Plenum Press, Murray Hill, NJ, 1983).
4. W. A. ZDANIEWSKI and H. P. KIRCHNER, *J. Amer. Ceram. Soc.* **70** (1987) 548.
5. J. B. HURST and S. DUTTA, *J. Amer. Ceram. Soc.* **70** (1987) C303.
6. H. KODAMA and T. MIYOSHI, *Adv. Ceram. Mater.* **3** (1988) 177.
7. T. B. JACKSON, A. C. HURFORD and S. L. BURNER, in "Silicon Carbide '87", edited by J. D. Cawley and C. E. Semler (The American Ceramic Society, Westerville, OH, 1987) p. 227.
8. R. A. CUTLER, J. D. BRIGHT, A. V. VIRKAR and D. K. SHETTY, *J. Amer. Ceram. Soc.* **70** (1987) 714.
9. R. SATHYAMOORTHY, A. V. VIRKAR and R. A. CUTLER, *J. Amer. Ceram. Soc.* **75** (1992) 1136.
10. J. DONGLIANG, S. JIHONG, T. SHOUHONG and P. GREIL, *J. Amer. Ceram. Soc.* **75** (1992) 2586.
11. O. J. KWON and D. N. YOON, in "Sintering and Related Phenomena", edited by G. C. Kuczynski (Plenum Publishing Company, NY, 1980) p. 203.
12. Y. S. KIM, J. K. PARK and D. N. YOON, *Int. J. Pow. Metall. Pow. Tech.* **21** (1985) 29.
13. Y. W. KIM and J. G. LEE, *J. Mater. Sci.* **27** (1992) 4746.
14. J. GURLAND, *J. Met.* **6** (1954) 285.
15. W. RAFANIELLO, K. CHO and A. V. VIRKAR, *J. Mater. Sci.* **16** (1981) 3479.
16. C. GRESKOVICH and J. H. ROSOLOWSKI, *J. Amer. Ceram. Soc.* **59** (1976) 336.
17. A. V. VIRKAR, J. L. HUANG and R. A. CUTLER, *J. Amer. Ceram. Soc.* **70** (1987) 164.
18. R. A. GIDDINGS, C. A. JOHNSON, S. PROCHAZKA and R. J. CHARLES, "Fabrication and properties of Sintered Silicon Carbide", G. E. Tech. Report, No 75CRD060, 1975.
19. J. B. WACHTMAN Jr, "Structural Ceramics" (Treatise on Materials Science and Technology, Vol 29, Academic Press, Boston, MA, 1989).
20. D. B. MARSHALL and B. R. LAWN, *J. Amer. Ceram. Soc.* **61** (1978) 21.

Received 30 September 1993
and accepted 27 July 1994